A MAC and Physical Layer Theoretical Model for IEEE 802.11a Networks Operating Simultaneously with Basic and RTS/CTS Access Schemes

Roger Pierre Fabris Hoefel

Department of Telecommunications Engineering - University La Salle
92010-000 - Canoas - RS - Brazil

roger@lasalle.tche.br

Abstract *— We have developed a theoretical cross-layer model that allows assessing the goodput and delay of the IEEE 802.11a local area networks (WLANs) operating simultaneously under the distributed coordination function (DCF) basic access (BA) and request-to-send/clear-to-send (RTS/CTS) medium access control (MAC) protocols under saturated traffic over correlated and uncorrelated fading channels.*

Resumo. *Neste artigo é proposto um modelo teórico que permite analisar de maneira integrada o desempenho das camadas de enlace e física de redes locais sem fio IEEE 802.11a operando simultaneamente no modo básico e no modo RTS/CTS. As expressões analíticas propostas, validadas por meio de simulação da camada física IEEE 802.11a, permitem verificar no desempenho do sistema tanto os efeitos dos protocolos de enlace (e.g. da carga no canal, do tamanho dos pacotes, do algoritmo de resolução da janela de contenção) bem como os efeitos dos protocolos da camada física (e.g. esquemas de modulação, correção de erros, modelos de canal).*

1. Introductions and Related Work

The release of the first IEEE 802.11 standard (that specifies the MAC and the original slower frequency-hopping and direct sequence PHY layers) in 1997 paved the way for a world wide development of a standardized cost-effective scalable technology for WLANs. Since then, intensive research activities have been carried out on analyze, design, implementation, and optimization issues of IEEE 802.11 networks. In 1997, B. P. Crow et al published one of the first papers to explain the IEEE 802.11 protocol (with particular emphasis on the MAC layer) and to show simulation results for packetized data and a combination of packetized data and voice over WLANs [Crow 1997]. In 2000, Bianchi proposed an analytical bi-dimensional Markov model to estimate the performance of IEEE 802.11 networks [BIANCHI 2000] operating under saturated traffic conditions over ideal channels (i.e. only collisions were taken into account and the frames were not corrupted due to noise and interference). This Bianchi's model has been used as a framework to analyze others IEEE 802.11 technologies, as in [Robinson 2004] where it is proposed an analytical model to assess the performance of quality of service (QoS) schemes for IEEE 802.11 WLANs operating under saturated traffic conditions over ideal channels. In 2002, Qiao et al [Qiao 2002] derived an analytical model that takes the non-ideal channel into account on the performance of IEEE802.11a WLANs. However, they assumed a very crude model for the MAC layer. Therefore, due to the properties of the radio channel and the use of advanced PHY layer techniques, there was a necessity to develop an accurate joint MAC and PHY theoretical

model to estimate the performance of IEEE802.11based networks. Hence, founded on the methodology proposed by Bianchi in [BIANCHI 2000], we have developed a cross-layer saturation goodput theoretical model that allows assessing the performance of IEEE 802.11a WLANs over uncorrelated [HOEFEL 2005] and correlated fading channels [HOEFEL 2006].

We have also noticed a lack in the literature on theoretical analyzes of IEEE 802.11 WLANS when both the BA and RTS/CTS access schemes are simultaneously operational, even when it is assumed an ideal PHY layer. Therefore, in the present contribution we have improved our previous theoretical results by: (1) developing a cross-layer model that allows to estimate the goodput and delay of IEEE 802.11a WLANs o*perating simultaneously under the basic and RTS/CTS access schemes*; *(2)* carrying out a unified comparison between the performance of IEEE 802.11a WLANs over uncorrelated and correlated fading channels when both access modes are simultaneously operational. The above contributions are developed in Sections 4 to 10. We remark that this developed cross-layer methodology can be used, with minor modifications, to examine the performance of other 802.11 PHY layers (e.g. 802.11b and 802.11g) as well as to be used as reference to analyze the effects of the PHY layer on MAC protocols for different systems (e.g. IEEE 802.16). In the next two sections we present meaningful aspects regarding to 802.11a MAC (Section 2) and PHY (Section 3) layers. The contributions of this work are developed in Sections 4 to 10.

2. IEEE 802.11 MAC

The IEEE PHY standards 802.11, 802.11a and 802.11b use the same MAC layer protocols. To accomplish it, a MAC service unit (MSDU) is segmented into a MAC protocol data unit (MPDU) that, on its turn, it is mapped to the physical layer using a standardized physical layer convergence procedure (PLCP). As the IEEE 802.11 MAC protocol is widely known, we only show at Figures 1a and 1b the time diagram for the atomic transmission used by the DCF BA and RTS/CTS mechanisms [Gast 2002]. Notice that DIFS stands for DCF interframe spacing (IFS), PIFS for point coordination IFS, SIFS for short IFS and NAV for network allocation vector.

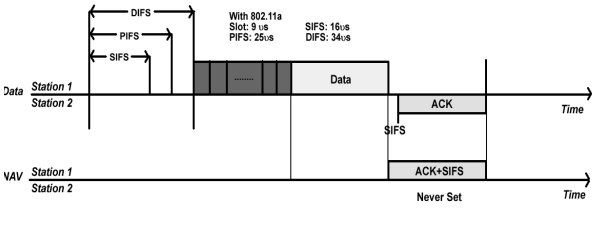

Fig. 1a. The atomic BA scheme.

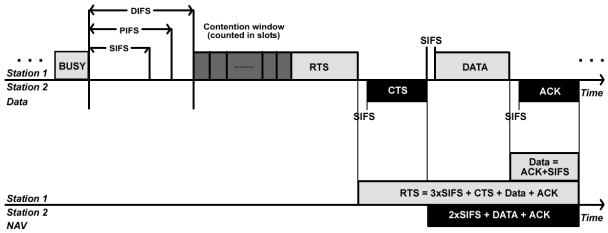

Fig. 1b. The atomic RTS/CTS scheme.

Figure 1. The atomic cycle for the successful transmission using the atomic basic positive ACK of data and RTS/CTS schemes.

3. IEEE 802.11 Physical Layer

In this paper we have followed the IEEE 802.11a PHY layer [IEEE 802.11a 1999, pp. 16]. The IEEE 802.11a is based on orthogonal frequency division modulation (OFDM)

using a total of 52 subcarriers, of which 48 subcarriers carry actual data and four subcarriers are pilots used to facilitate coherent detection. The channel symbol rate R_s is of *12 Msymbols/sec* since the OFDM symbol interval (*tS)* is set to 4μs. Tab. 1 shows the OFDM PHY modes, where *BpS* means Bytes per Symbol. For instance, the *PHY mode 1* carries 3 bytes per symbol, i.e. 6 Mbps* *tSymbol/8.0=3 BpS*.

Tab. 1. The IEEE 802.11a PHY modes.

Mode p	*Modulation*	*Code Rate R_c*	*Data Rate*	*BpS*
1	BPSK	1/2	6 Mbps	3
2	BPSK	3/4	9 Mbps	4.5
3	QPSK	1/2	12 Mbps	6
4	QPSK	3/4	18 Mbps	9

Mode p	*Modulation*	*Code Rate R_c*	*Data Rate*	*BpS*
5	16-QAM	1/2	24 Mbps	12
6	16-QAM	3/4	36 Mbps	18
7	64-QAM	2/3	48 Mbps	24
8	64-QAM	3/4	54 Mbps	27

Considering the IEEE 802.11a convolutional codes generator polynomials, $\boldsymbol{g_0}=(133)_8$ and $\boldsymbol{g_1}=(171)_8$, of rate $r=1/2$ and constrain length $K=7$, then the union bound on the probability of decoding error is given by [Conan 1984]

$$P_e(\gamma_b,p)<11P_{10}(\gamma_b,p)+38P_{12}(\gamma_b,p)+193P_{14}(\gamma_b,p)+\cdots \quad (1)$$

where the used notation emphasizes the dependence of P_d with the received signal-to-interference-plus-noise (SINR) per bit γ_b, and the *PHY mode p*. The union bound on the probability of decoding error for the higher code rates of 2/3 and 3/4 (which are obtained by puncturing the original rate-1/2 code), are given by (2) and (3), respectively [Haccoun 1989].

$$P_e(\gamma_b,p)<P_6(\gamma_b,p)+16P_7(\gamma_b,p)+48P_8(\gamma_b,p)+\cdots \quad (2)$$

$$P_e(\gamma_b,p)<8P_5(\gamma_b,p)+31P_6(\gamma_b,p)+160P_7(\gamma_b,p)+\cdots \quad (3)$$

Assuming that the convolutional forward error correcting code (FEC) is decoded using hard-decision Viterbi decoding, then (4-5) model the probability of selecting incorrectly a path when the Hamming distance d is even and odd, respectively. The average bit error rate (BER) for the *PHY mode p* modulation scheme is denoted by ρ_p.

$$P_d(\gamma_b,p)=\frac{1}{2}\binom{d}{d/2}p_p^{d/2}(1-\rho_p)^{d/2}+\sum_{k=d/2+1}^{d}\binom{d}{k}\rho_p^k(1-\rho_p)^{d-k} \quad (4)$$

$$P_d(\gamma_b,p)=\sum_{k=(d+1)/2}^{d}\binom{d}{k}\rho_p^k(1-\rho_p)^{d-k} \quad (5)$$

The number of octets of the PHY layer protocol data unit (PDU) for the RTS frame is given by

$$N_{rts}=N_{pre}+N_{srv}+l_{rts}+N_{tail}=3+\frac{16}{8}+20+\frac{6}{8} \quad (6)$$

where N_{pre}, N_{srv} and N_{tail} denote the number of octets of the preamble, service and tail fields, respectively. The number of octets used to carry the "logical control information" sent by the RTS, CTS and ACK control frames is labelled by l_{rts}, l_{cts} and l_{ack}, respectively.

The number of octets of the PPDU that transports the CTS and ACK control frames is given by (7), where $l=l_{cts}=l_{ack}=14$ *octets.* The MAC PCLP PDU (i.e. a PPDU) length is given by (8), where l_{pl} denotes the payload length in octets. The MPDU header and the cyclic redundant checking (CRC) fields have together a size of 34 bytes [GAST 2002] and 6 bits are used to flush out the convolutional coder to the zero state.

$$N_{cts}=N_{ack}=N_{pre}+N_{srv}+l+N_{tail}=3+\frac{16}{8}+14+\frac{6}{8} \quad (7)$$

$$N_{mp}=N_{pre}+N_{srv}+N_{mh}+N_{pl}+N_{tail}=3+\frac{16}{8}+34+l_{pl}+\frac{6}{8} \quad (8)$$

The time period spent to transmit a MPDU with a payload of l_{pl} *octets* over the IEEE 802.11a using the *PHY mode* p_{mp} is given by (9). The length of RTS, CTS and ACK control frames are given by (10-12), respectively.

$$T_{mp}(p_{mp}) = tPCLP\_\mathrm{Pre} + tPCLP\_SIG + \left\lceil \frac{l_{pl} + 34 + (16+6)/8}{BpS(p_{mp})} \right\rceil \cdot tS \quad (9)$$

$$T_{rts}(p_{rts}) = tPCLP\_\mathrm{Pre} + tPCLP\_SIG + \left\lceil \frac{l_{rts} + (16+6)/8}{BpS(p_{rts})} \right\rceil \cdot tS \quad (10)$$

$$T_{cts}(p_{cts}) = tPCLP\_\mathrm{Pre} + tPCLP\_SIG + \left\lceil \frac{l_{cts} + (16+6)/8}{BpS(p_{cts})} \right\rceil \cdot tS \,. \quad (11)$$

$$T_{ack}(p_{ack}) = tPCLP\_\mathrm{Pre} + tPCLP\_SIG + \left\lceil \frac{l_{ack} + (16+6)/8}{BpS(p_{ack})} \right\rceil \cdot tS \quad (12)$$

4. Analytical Results for the Saturation Goodput

It is assumed a fixed number of *n* STAs operating in saturation conditions, i.e. each STA has a packet to transmit after the completion of each successful transmission. It is also postulated that each packet collides with a constant and independent *conditional collision probability p.* The capture effect is neglected in such way that the lost of frames due to collisions is independent of the lost of frames due to noise and interference. The post backoff procedure has not been taken into account [Robison 2004].

The probability that a transmitted MPDU is successful depends upon the following events: *(1)* no collision and successful transmission using the BA scheme; *(2)* no collision and successful transmission using the RTS/CTS access scheme. Thus,

$$P_s = (1-p) \cdot \left\{ P_{ba} \cdot \left(S_{mp} \cdot S_{ack} \right) + P_{rts} \cdot \left(S_{rts} \cdot S_{cts} \cdot S_{mp} \cdot S_{ack} \right) \right\} \quad (13)$$

where $S_{cts,}$ S_{rts} and S_{ack} denote, respectively, the probability that the RTS, CTS and ACK control frames be transmitted with success. S_{mp} denotes the probability the transmission of a MPDU frame is successful.

Eq. (14) and (15) model the probability that a MPDU is transmitted using the basic access and RTS/CTS schemes, respectively. Notice that these probabilities depend upon the MAC payload length l_{pl} and the *RTSThreshold* defined at the Management Information Base (MIB).

$$P_{ba} = Pr\left\{ l_{pl} < RTSThreshold \right\} \quad (14) \qquad P_{rts} = Pr\left\{ l_{pl} \geq RTSTheshold \right\} \quad (15)$$

Eq. (16) details the events that cause an unsuccessful MPDU transmission: *(1)* collision; *(2)* no collision, but a corrupted frame on the basis access scheme (see 17); *(3)* no collision, but a corrupted frame on the RTS/CTS access scheme (see 18).

$$P_f = p + (1-p) \cdot \left(P_{ba} \cdot P_{f,ba} + P_{rts} \cdot P_{f,rts} \right) \quad (16)$$

$$P_{f,ba} = (1 - S_{mp}) + S_{mp} \cdot (1 - S_{ack}) = 1 - S_{mp} \cdot S_{ack} \quad (17)$$

$$P_{f,rts} = \left[(1 - S_{rts}) + S_{rts}(1 - S_{cts}) + S_{rts} \cdot S_{cts} \cdot (1 - S_{mp}) + S_{rts} S_{cts} \cdot S_{mp}(1 - S_{ack}) \right] = 1 - S_{rts} \cdot S_{cts} \cdot S_{mp} \cdot S_{ack} \quad (18)$$

Fig. 2 shows a discrete bi-dimensional Markov chain *(s(t),b(t))* for the backoff window size. It is assumed that: *(1)* a MPDU is transmitted using the basic access scheme with probability $P_{ba.}$; *(2)* a MPDU is transmitted using the RTS/CTS scheme with probability P_{rts}; *(3) s(t)* is the stochastic process of the backoff stage *(0,⋯,m)* of the STA at time *t,* where *m* denotes the number of backoff stages; *(4) b(t)* is the random

process that models the backoff time counter for a given STA; *(5)* the contention window (CW) size at backoff stage *i* is labeled as $W_i = 2^i W$, where $i \in (0,m)$ is the backoff stage and *W* is the MAC CW size parameter CW_{min} The maximum CW size is denoted as $W_m = 2^m W - 1 = CW_{max} - 1$.

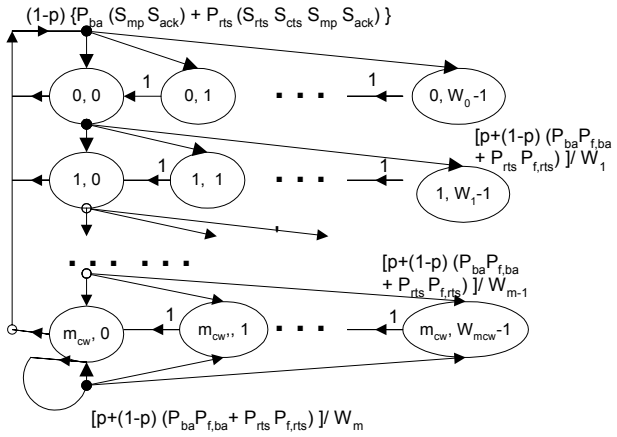

Figure 2. Bi-dimensional Markov chain *(s(t),b(t))* model for the backoff window size and a non-ideal channel.

4.1. Packet Transmission Probability

Using the notation $P\{i_1,k_1/i_0,k_o\} = P\{s(t+1)=i_1, b(t+1)=k_1 \mid s(t)=i_o, b(t)=k_o\}$, equations (19) to (22) model the null one-step transition probabilities of the bi-dimensional Markov chain depicted at Fig. 2. The decreasing of the backoff timer at the beginning at each slot time of size σ is modeled as

$$P\{i,k \mid i,k+1\} = 1 \quad for \;\; k \in (0, W_i - 2) \;\; and \;\; i \in (0,m) \tag{19}$$

Eq. (20) takes into account that a new PPDU starts at the backoff stage 0 and that the backoff is uniformly distributed into the range *(0, W_0-1)* after a successful PPDU transmission.

$$P\{0,k \mid i,0\} = [1-p] \cdot \begin{bmatrix} P_{ba} \cdot (S_{mp} \cdot S_{ack}) + \\ P_{rts} \cdot (S_{rts} \cdot S_{cts} \cdot S_{mp} \cdot S_{ack}) \end{bmatrix} / W_0 \;\; for \;\; k \in (0, W_0 - 1) \;\; and \;\; i \in (0,m) \tag{20}$$

The property that a new backoff value is uniformly chosen in the range *(0,W_i)* after an unsuccessful transmission at the backoff stage *i-1* can be modeled as

$$P\{i,k \mid i-1,0\} = \{p + [1-p] \cdot \begin{bmatrix} P_{ba} \cdot (1 - S_{mp} \cdot S_{ack}) + \\ P_{rts} \cdot (1 - S_{rts} \cdot S_{cts} \cdot S_{mp} \cdot S_{ack}) \end{bmatrix} \} / W_i \; for \; k \in (0, W_i) \;\; and \;\; i \in (1,m) \tag{21}$$

Eq. (22) models the fact that the backoff is not increased in subsequent frame transmissions once the backoff stage has reached the value *m*.

$$P\{m,k \mid m,0\} = \{p + [1-p] \cdot [P_{ba} \cdot (1 - S_{mp} \cdot S_{ack}) + P_{rts} \cdot (1 - S_{rts} \cdot S_{cts} \cdot S_{mp} \cdot S_{ack})] \} / W_m \;\; for k \in (0, W_{mi} - 1) \tag{22}$$

The transmission occurs when the backoff timer counter is equal to zero. Therefore, using an algebraic procedure similar to the one developed in [Hoefel 2005], then we can show that the probability that a STA transmits in a randomly chosen slot time is given by (23), where, the stationary probability of a given STA be in the time

slot 0 for first contention window is given by (24). The average frame success transmission probability is denoted by (25).

$$\tau = \sum_{i=0}^{m} b_{i,0} = \frac{b_{0,0}}{(1-p)\cdot\left[P_{ba}\cdot\left(S_{mp}\cdot S_{ack}\right)+P_{rts}\cdot\left(S_{rts}\cdot S_{cts}\cdot S_{mp}\cdot S_{ack}\right)\right]} \tag{23}$$

$$b_{0,0} = \frac{2\cdot(1-p)\cdot S\cdot[1+2\cdot S\cdot(p-1)]}{1+2^{m}W\cdot[1+(-1+p)\cdot S]^{m}+(-1+p)\cdot S\cdot\left\{2+W+2^{m}W\cdot[1+(-1+p)\cdot S]^{m}\right\}} \tag{24}$$

$$S = P_{ba}\cdot\left(S_{mp}\cdot S_{ack}\right)+P_{rts}\cdot\left(S_{rts}\cdot S_{cts}\cdot S_{mp}\cdot S_{ack}\right) \tag{25}$$

Notice that for an ideal channel (i.e. $S_{rts}=S_{cts}=S_{mp}=S_{ack}=1$), Eq. (24) resumes to

$$b_{0,0} = \frac{2(1-2p)\cdot(1-p)}{(1-2p)\cdot(W+1)+pW\cdot\left[1-(2p)^{m}\right]} \tag{26}$$

which is in agreement with (6) of [Bianchi 2000].

Each STA transmits with probability τ. Therefore, the conditional probability that a transmitted PPDU encounters a collision in a given slot time can be stated as

$$p = 1-(1-\tau)^{n-1}. \tag{27}$$

The nonlinear system represented by (23) and (27) can be solved using numerical techniques.

4.2 Goodput

The goodput (net throughput) in *bits per second (bps)* can be modeled as the ratio of the payload bits transmitted with success to the average cycle time, i.e.

$$G_{bps} = \frac{P_{ba}\cdot\overline{N}_{ba}+P_{rts}\cdot\overline{N}_{rts}}{P_{ba}\cdot\overline{T}_{ba}+P_{rts}\cdot\overline{T}_{rts}} \tag{28}$$

The average number of payload bits transmitted with success for the BA and RTS/CTS schemes are given by (29) and (30), respectively. The number of payload octets when is used the BA and RTS/CTS schemes are given by $l_{pl,ba}$ and $l_{pl,rts}$, respectively.

$$\overline{N}_{ba} = 8\cdot l_{pl,ba}\cdot P_s\cdot P_{tr}\cdot S_{mp}\cdot S_{ack} \tag{29}$$

$$\overline{N}_{rts} = 8\cdot l_{pl,rts}\cdot P_s\cdot P_{tr}\cdot S_{rts}\cdot S_{cts}\cdot S_{mp}\cdot S_{ack} \tag{30}$$

The probability that there is no collision on the channel conditioned to the fact that at least one STA transmits is given by

$$P_s = \frac{\binom{n}{1}\cdot\tau\cdot(1-\tau)^{n-1}}{P_{tr}} = \frac{n\cdot\tau\cdot(1-\tau)^{n-1}}{P_{tr}} = \frac{n\cdot\tau\cdot(1-\tau)^{n-1}}{1-(1-\tau)^{n}} \tag{31}$$

where P_{tr} is the probability that there is at least one transmission in the considered slot time. The average cycle time for the basic access and RTS/CTS scheme is given by (32) and (33), respectively.

$$\overline{T}_{ba} = \overline{B}_{s,ba}+\overline{B}_{f1,ba}+\overline{B}_{f2,ba}+\overline{B}_{f3,ba}+\overline{I} \tag{32}$$

$$\overline{T}_{rts} = \overline{B}_{s,rts}+\overline{B}_{f1,rts}+\overline{B}_{f2,rts},+\overline{B}_{f3,rts}+B_{f4,rts}+B_{f5,rts}+\overline{I} \tag{33}$$

For the basic access scheme, the average busy time when the atomic positive ACK basic access transmission is successful is given by

$$\overline{B}_{s,ba} = P_s\cdot P_{tr}\cdot S_{mp}\cdot S_{mac}\cdot\left(DIFS+T_{mp}\left(p_{mp}\right)+a+SIFS+T_{ack}(p_{ack})+a\right) \tag{34}$$

where a is the propagation delay. $T_{mp}(p_{mp})$ is the time period necessary to transmit a MPDU when it is used the *PHY mode* p_{mp} (see 9), and $T_{ack}(p_{ack})$ is the time period spent to transmit a positive ACK control frame using the PHY mode p_{ack} (see 12).

The average busy time when the transmission is successful using the RTS/CTS scheme is given by

$$\overline{B}_{s,rts} = P_s \cdot P_{tr} \cdot S_{rts} \cdot S_{cts} \cdot S_{mp} \cdot S_{mac} \cdot [DIFS + T_{rts}(p_{rts}) + a + SIFS + T_{cts}(p_{cts}) + a + SIFS + T_{mp}(p_{mp}) + a + SIFS + T_{ack}(p_{ack}) + a] \quad (35)$$

where $T_{rts}(p_{rts})$, $T_{cts}(p_{cts})$ and denote the time necessary to transmit the RTS and CTS control frames when it is used the *PHY mode* p_{rts} and p_{cts}, respectively (see 10 and 11).

$\overline{B}_{f1,ba}$ models the average amount of time that the channel is busy due to collisions of a MPDU frames when it used the BA scheme (see 36). However, for the RTS/CTS MAC scheme the waste time occurs due to RTS control frame collisions, as modeled by $\overline{B}_{f1,rts}$ (see 37).

$$\overline{B}_{f1,ba} = P_{tr} \cdot (1 - P_s) \cdot (DIFS + T_{mp}(p_{mp}) + a) \quad (36)$$

$$\overline{B}_{f1,rts} = P_{tr} \cdot (1 - P_s) \cdot (DIFS + T_{rts}(p_{rts}) + a) \quad (37)$$

$\overline{B}_{f2,ba}$ and $\overline{B}_{f3,ba}$ model the average lost time due to an unsuccessful transmission of data and ACK control frames, respectively, when it is used the BA scheme.

$$\overline{B}_{f2,ba} = P_{tr} \cdot P_s \cdot (1 - S_{mp}) \cdot (DIFS + T_{mp}(p_{mp}) + a) \quad (38)$$

$$\overline{B}_{f3,ba} = P_{tr} \cdot P_s \cdot S_{mp} \cdot (1 - S_{ack}) \cdot \begin{pmatrix} DIFS + T_{mp}(p_{mp}) + a + \\ SIFS + T_{ack}(p_{ack}) + a \end{pmatrix} \quad (39)$$

$\overline{B}_{f2,rts}$, $\overline{B}_{f3,rts}$, $\overline{B}_{f4,rts}$ and $\overline{B}_{f5,rts}$ model the average time that the channel is busy with unsuccessful transmissions due to noise and interference, of RTS, CTS, data and ACK frames, respectively, when it is used the RTS/CTS access scheme. Finally, the average time that a slot time is idle is given by (39), where σ is the slot time length.

$$\overline{B}_{f2,rts} = P_{tr} \cdot P_s \cdot (1 - S_{rts}) \ [DIFS + T_{rts}(p_{rts}) + a] . \quad (40)$$

$$\overline{B}_{f3,rts} = P_{tr} \cdot P_s \cdot S_{rts} \cdot (1 - S_{cts}) [DIFS + T_{rts}(p_{rts}) + a + SIFS + T_{cts}(p_{cts}) + a]. \quad (41)$$

$$\overline{B}_{f4,rts} = P_{tr} \cdot P_s \cdot S_{rts} \cdot S_{cts} \cdot (1 - S_{mp}) [DIFS + T_{rts}(p_{rts}) + a + SIFS + T_{rcs}(p_{cts}) + a + SIFS + T_{mp}(p_{mp}) + a] \quad (42)$$

$$\overline{B}_{f5,rts} = P_{tr} \cdot P_s \cdot S_{rts} \cdot S_{mp} \cdot (1 - S_{ack}) [DIFS + T_{rts}(p_{rts}) + a + SIFS + T_{rcs}(p_{cts}) + a + SIFS + T_{mp}(p_{mp}) + a + SIFS + T_{ack}(p_{ack}) + a] \quad (43)$$

$$\overline{I} = (1 - P_{tr}) \cdot \sigma \ . \quad (44)$$

5. Analytical Results: Average Delay

The average delay between the time that a MPDU arrived at the queue until the time that an ACK for this MPDU is received can be modeled as the average number of cycle times necessary to accomplish a successful MPDU transmission, as modeled by (45). The average cycle time for the BA and RTS/CTS schemes is given by (32) and (33), respectively. The average number of time slots spent for a successful transmission is given by (46), where the average probability that an atomic transmission is not successful, P_f, is given by (16).

$$\overline{\overline{D}} = \overline{P} \cdot \left\{ P_{ba} \cdot \overline{T}_{ba} + P_{rts} \cdot \overline{T}_{rts} \right\} \quad (45) \qquad \overline{P} = \sum_{i=0}^{m-1} \left[(P_f)^i \frac{W_i}{2} \right] + \sum_{i=m}^{\infty} \left[(P_f)^i \cdot \frac{W_m}{2} \right] \quad (46)$$

6. Analytical Results for Frame Success Probability over Uncorrelated Fading Channels

In order to have a unified analytical framework upon the modeling of fading effects on the MAC protocols we have summarized in this Section the theoretical results developed in [Hoefel 2005]. We believe that this approach is time saving to the reader.

Postulating that the errors inside of the decoder are interdependent, then the upper bound for a successful transmission of a frame with *l* octets is given by (47) [Puersley 1987]. Notice that the union bound on the probability of decoding error is given by: *(1)* Eq. (1) for the PHY modes 1, 3 and 5; *(2)* Eq. (2) for the PHY mode 7; *(3)* Eq. (3) for the PHY modes 2, 4, 6 and 8.

$$S(l, \gamma_b, p) < \left[1 - P_e(\gamma_b, p) \right]^{8l} \quad (47)$$

The PCLP header is always transmitted using PHY mode 1. Then, for an uncorrelated multipath fading channel, the successful MPDU transmission when it is used the PHY mode p_{mp} is given by (48). Correspondingly, the RTS, CTS and ACK control frames success probabilities are given by (49), (50) and (51), respectively.

$$S_{mp}(l_{mp}, \gamma_b, p_{mp}) = S(24/8, \gamma_b, 1)\, S(34 + (16+6)/8 + l_{mp}, \gamma_b, p_{mp}) \quad (48)$$

$$S_{rts}(l_{rts}, \gamma_b, \rho_{rts}) = S(24/8, \gamma_b, 1)\, S(20 + (16+6)/8, \gamma_b, \rho_{rts}) \quad (49)$$

$$S_{cts}(l_{cts}, \gamma_b, \rho_{cts}) = S(24/8, \gamma_b, 1)\, S(14 + (16+6)/8, \gamma_b, \rho_{cts}) \quad (50)$$

$$S_{ack}(l_{ack}, \gamma_b, \rho_{ack}) = S(24/8, \gamma_b, 1)\, S(14 + (16+6)/8, \gamma_b, \rho_{ack}) \quad (51)$$

In this subsection we have assumed a flat fading Nakagami-m channel temporally independent at symbol level and independent across of the OFDM carriers. Therefore, the average BER for the *PHY mode p* can be stated as

$$\rho_p = \int_0^{\infty} P_p(\gamma_b, p)\, p(\gamma_b) d\gamma_b \quad (52)$$

where the $P_p(\gamma_b)$ is a function that depends on the signal-to-noise-plus-interference ratio (SINR)γ_b, the modulation/coding scheme p, the receiver structure and the channel. Considering a maximum ratio combining (MRC) receiver matched with the channel diversity and that the same average power Ω is received at each diversity branch, then the probability distribution function (pdf) of the SINR per bit at the Viterbi decoder input is of gamma kind [Hoefel 2005], i.e.

$$p(\gamma_b) = \frac{1}{\Gamma(L\, m_n)} \left(\frac{m_n}{\bar{\gamma}_b} \right)^{L m_n} (\gamma_b)^{L m_n - 1} \exp\left(- \frac{m_n \gamma_b}{\bar{\gamma}_b} \right) \quad if \;\; \gamma_b > 0,\; m_n \geq 0.5 \quad (53)$$

where m_n is the fading figure, $\bar{\gamma}_b$ is the average SINR per bit at the detector output (or at Viterbi decoder input) and *L* is the number of diversity branches. Notice that $m_n = 1$ models a Rayleigh channel.

For binary phase-shift keying (BPSK used in PHY modes 1 and 2) and quaternary PSK (QPSK used in PHY modes 3 and 4) signaling schemes, then the BER is given by [Proakis 2001, pp. 269]

$$P_p(\gamma_b, p) = Q\left(\sqrt{2\gamma_b R_c}\right) \text{ for } p = 1,2,3,4, \quad (54)$$

where R_c is the code rate and $Q(x)$ is the complementary Gaussian cumulative distribution function.

For rectangular M-ary quadrature amplitude modulation (M-QAM signaling used in PHY modes 5, 6, 7 and 8), $P_p(\gamma_b)$ is given by by (55), where M is the cardinality of the modulation and $erfc(z)$ is the complementary error function and $p=5, 6, 7$ and 8 [Yang 2000].

$$P_p(\gamma_b, p) = \frac{\sqrt{M}-1}{\sqrt{M}\ log_2\sqrt{M}} erfc\left(\sqrt{\frac{2log_2 M \cdot \gamma_b \cdot R_c}{2(M-1)}}\right) + \frac{\sqrt{M}-2}{\sqrt{M}\ log_2\sqrt{M}} erfc\left(\sqrt{\frac{3log_2 M \cdot \gamma_b \cdot R_c}{2(M-1)}}\right). \quad (55)$$

7. Analytical Results for Frame Success Probability over Block Correlated Fading Channels

Here, we have assumed that the fading is correlated at each atomic cycle (see Fig. 1 and 2) and uncorrelated among distinct atomic cycles. As stated for uncorrelated fading channels, the union bound on the probability of decoding error is given by: *(1)* Eq. (1) for the PHY modes 1, 3 and 5; *(2)* Eq. (2) for the PHY mode 7; *(3)* Eq. (3) for the PHY modes 2, 4, 6 and 8.

Assuming that the errors inside of the hard decision Viterbi decoder are interdependent, then *Pursley* and *Taipale* have shown that the upper bound for a successful transmission of a frame with l octets is given by [Puersley 1987]

$$S(l, \gamma_b, m) < \left[1 - P_e(\gamma_b, m)\right]^{8l} \quad (56)$$

For a block-fading channel, this upper bound may be modified to (57a), where the $p(\gamma_b)$ is the pdf of the SINR per bit at the demodulator output (e.g. $p(\gamma_b)$ is given by (53) for MRC receiver over a Nakagami-m fading channel) and γ_{inf} is chosen to satisfy the inequality (57b).

$$S(l, \gamma_b, p) < \int_{\gamma_{inf}}^{\infty} [1 - Pe(\gamma_b, p)]^{8l} p(\gamma_b) d\gamma_b \qquad 1 - Pe(\gamma_{\inf}, p) \le 1. \quad (57a,b)$$

7.1 PHY Mode 1 (BPSK@6Mbps)

For the *PHY mode 1*, the union bound on the decoding error can be estimated using (1) and (4), where ρ_m is given by (58) with $R_c=1/2$.

$$\rho_1 = P_p(\gamma_b) = Q\left(\sqrt{2\gamma_b R_c}\right). \quad (58)$$

Since all frames are transmitted using the *PHY mode 1*, then S_{rts}, S_{cts}, S_{mp} *and* S_{ack} can be estimated using (59-65) with $p=1$.

$$S_{rts}(p_{rts}) = S(N_{rts}, \gamma_b, p_{rts}); \quad (59)$$

$$S_{cts}(p_{cts}) = P\{CTS\ is\ ack\ /\ RTS\ was\ ack\}; \quad (60)$$

$$S_{cts}(p_{cts}) = \frac{S(N_{rts} + N_{cts}, \gamma_b, p_{cts})}{S_{rts}}; \quad (61)$$

$$S_{mp}(p_{mp}) = P\{MPDU \text{ is correct} / \text{RTS, CTS were correct}\}; \quad (62)$$

$$S_{mp}(p_{mp}) = \frac{S(N_{rts} + N_{cts} + N_{mp}, \gamma_b, p_{mp})}{S_{rts} S_{cts}}; \quad (63)$$

$$S_{ack}(p_{ack}) = P\{ACK \text{ is correct} / RTS, \text{CTS, MPDU were correct}\} \quad (64)$$

$$S_{ack}(p_{ack}) = \frac{S(N_{rts} + N_{cts} + N_{mp} + N_{ack}, \gamma_b, p_{ack})}{S_{rts} S_{cts} S_{mp}}. \quad (65)$$

7.2 PHY Mode 2 (BPSK@9Mbps)

When the MPDU is transmitted using the *PHY mode 2*, then all control frames are transmitted using the *PHY mode 1*. Thus, the S_{rts} and S_{cts} are still given by (59) and (61) with $p=1$. The union bound on the decoding error can be estimated using (3) and (5), where ρ_m is given by (58) with $R_c=3/4$. The S_{md} can be stated as

$$S_{mp}(2) \cong \frac{S(36.75 + N_{mp}, \gamma_b, 2)}{S_{rts}(1) S_{cts}(1)} = \frac{S(36.75 + N_{mp}, \gamma_b, 2)}{S(N_{rts} + N_{cts}, \gamma_b, 1)} \quad (66)$$

Notice that the 3 octets of the preamble were not taken into account in (66) since they are transmitted using the PHY mode 1 (i.e. a more robust modulation scheme). We also have used the following approximation:

$$P\{MPDU \text{ is ack / RTS and CTS were ack}\} = \frac{P\{MPDU, RTS, CTS\}}{P\{RTS, CTS\}} \approx \frac{P\{MPDU\}}{P\{RTS, CTS\}} \quad (67)$$

since $N_{mp} >> (N_{rts}+N_{cts})$, and the MPDU is transmitted using the *PHY mode 2* (i.e. a signaling scheme with lesser immunity to noise and interference than the signaling scheme used to transmit the control frames).

The ACK control frame is transmitted using the *PHY mode 1*, while the MPDU is transmitted using the *PHY mode 2* (i.e. a signaling scheme more suitable to the decoding errors). Thus, the ACK control frame success probability can be approximated by (68) for block fading channels.

$$S_{ack}(m) = P\{ACK \text{ is ack / RTS, CTS and MPDU were ack}) \cong 1 \quad (68)$$

7.3 PHY Mode 3(QPSK@12Mbps)

In this case all control and data frames are transmitted using the PHY mode 3. Therefore, S_{rts} and S_{cts} are given by (59) and (61), respectively, with $p=3$. Correspondingly, S_{md} and S_{ack} are given by (63) and (65) with $p=3$. The union bound on the decoding error can be estimated using (1) and (4), where ρ_p given by (58) with $R_c=1/2$ for coherent demodulation [Proakis 2000].

7.4 PHY Mode 4 (QPSK@18Mbps)

Here, all the control frames are transmitted using the PHY mode 3 and the MPDU is transmitted using the PHY mode 4. Consequently, S_{rts} and S_{cts} are given by (59) and (61), respectively, with $p=3$. Using similar reasoning developed for PHY mode 2, then S_{md} is given by (69) and S_{ack} is given by (68). The union bound on the decoding error can be estimated using (3) and (5), where ρ_p given by (58) with $R_c=3/4$ for coherent demodulation [Proakis 2000].

$$S_{mpd}(4) \cong \frac{S(36.75 + N_{mpd}, \gamma_b, 4)}{S_{rts}(3) S_{cts}(3)} = \frac{S(36.75 + N_{mpd}, \gamma_b, 4)}{S(N_{rts} + N_{cts}, \gamma_b, 3)}. \quad (69)$$

7.5 PHY Mode 5 (16QAM@24Mbps)

In this case all control and data frames are transmitted using the PHY mode 5. Therefore, S_{rts} and S_{cts} are given by (59) and (61), respectively, with $p=5$. Correspondingly, S_{md} and S_{ack} are given by (63) and (65) with $p=5$. The union bound on the decoding error can be estimated using (1) and (4), where ρ_p for QAM signaling is given by (55) with $M=16$ and $R_c=1/2$.

7.6. PHY Mode 6 (16QAM@36Mbps), PHY Mode 7 (64QAM@48Mbps) and PHY Mode 8(64QAM@64Mbps)

For all these PHY modes the control frames are transmitted using the PHY mode 5 and the MPDU is transmitted using the PHY modes 6, 7, or 8. Thus, the S_{rts} and S_{cts} are still given by (59) and (61) with $p=5$. The S_{md} is given by

$$S_{mpd}(p) \cong \frac{S(36.75 + N_{mpd}, \gamma_b, p)}{S_{rts}(5) S_{cts}(5)} = \frac{S(36.75 + N_{mpd}, \gamma_b, p)}{S(N_{rts} + N_{cts}, \gamma_b, 5)} \tag{70}$$

where $p=6, 7$ and 8. The S_{ack} can be estimated by (68) since the control frames are transmitted using 16QAM with $R_c=1/2$ while the MPDU is transmitted using 16QAM with $R_c=3/4$ *(PHY 6)*, 64QAM with $R_c=2/3$ *(PHY 7)* or 64QAM with $R_c=3/4$ *(PHY 8)*.

8. Joint Link and Physical Layer IEEE 802.11 Simulator

The C^{++} 802.11a joint MAC and PHY layer has the following main characteristics:

- It implements the MAC state machine that fulfills the DCF BA and RTS/CTS MAC schemes (Fig. 1).
- The OFDM PHY layer is implemented assuming perfect synchronism. The PHY layer signal processing algorithms implements the maximum-likelihood hard decision detection for the PHY mode 1 to PHY mode 8.
- The convolutional hard-decision decoding is implemented using a semi-analytic approach as follows. The average BER is estimated at a frame basis using on-line statistics collected at the demodulator output. Then the average BER is used in (4-5) to estimate the probability of the successful MPDU transmission.
- It is assumed the following parameters: *slot time* $\sigma=9\mu S$, *SIFS=16* μs, *DIFS=EIFS=34* μs, $CW_{min}=16$, $CW_{max}=1023$, $m=6$, $a=1\mu.s$, $N_{pl}=1023$ *octets*. It is used a confidence interval of 98% [Hoefel 2005]

9. Analytical and Simulation Results: a Comparative Approach

In this section, assuming correlated and uncorrelated flat fading Rayleigh channels, we shall show results for the following system configurations: *(1)* IEEE 802.11a networks operating under the RTS/CTS access scheme ($P_{ba}=0$ and $P_{rts}=1$ in (13) and subsequent equations); *(2)* IEEE 802.11a networks operating under the basic access mode ($P_{ba}=1$ and $P_{rts}=0$ in (13) and in the following); *(3)* joint operation of basic and RTS/CTS schemes with $P_{ba}= P_{rts}=0.5$ in (13) and in the following. Unless otherwise noticed, l_{pl} is set to *1023 octets.*

9.1 Single Operation of Basic Mode Scheme and RTS/CTS Access Schemes Over Uncorrelated Fading Channel

Some results on the joint link and physical layer performance of IEEE 802.11a networks over uncorrelated mulitpath fading channel can be found in [Hoefel 2005], where we investigated the system performance assuming that <u>only</u> the RTS/CTS mechanism is

active. In this subsection, we complement the results shown in the [Hoefel 2005] comparing the goodput and delay performance of both access methods in relation to the PHY mode and payload length. Tab. 2 shows the maximum goodput and the minimum delay for the basic access and RTS/CTS schemes. For a payload of 1023 octets, we have noticed that when a modulation with low cardinality is used to transmit a MPDU, then a superior performance is attainable with the MAC RTS/CTS scheme since the minor time spent with collisions counterbalances the greater overhead due to the control frames. However, for a payload of 255 octets the maximum system performance is always obtained with the basic access scheme due to the lesser MAC overhead.

Tab. 2. Maximum goodput and minimum delay for the basic access and RTS/CTS schemes: N_{pl}=1023 and 255 octets.

Mode p	Max. Goodput (Mbps)				Min. Delay (ms)			
	255 octects		1023 octects		255 octects		1023 octects	
	BA	RTS/CTS	BA	RTS/CTS	BA	RTS/CTS	BA	RTS/CTS
1	3.2	3.1	4.1	4.8	6.3	6.5	19.5	16.8
2	4.2	3.8	6.0	6.7	4.8	5.4	13.6	12.2
3	5.2	4.7	7.8	8.8	3.9	4.3	10.5	9.5
4	6.7	5.5	11.0	11.8	3.0	3.7	7.4	7.1
5	8.0	6.4	14.0	14.3	2.5	3.2	5.8	5.7
6	9.6	7.2	18.8	18.0	2.1	2.8	4.3)	4.5
7	10.6	7.6	22.9	20.7	1.9	2.7	3.6	3.9
8	11.0	7.7	24.62	21.8	1.8	2.6	3.3	3.8

9.2 Comparison of the Performance of RTS/CTS Scheme Over Correlated Fading and Uncorrelated Fading Channel

Fig 3 shows that for temporally uncorrelated fading channel there is a well-defined short range of SINR per bit where the system performance is acceptable. On the other hand, when the fading is strongly correlated there is a wide and smooth variation of the goodput with the average SINR per bit. Fig. 3 also shows that the spatial diversity (assumed uncorrelated) provides greater gain in the required γ_b on environments where the fading is uncorrelated. However, the diversity gain is also substantial on temporally correlated fading environments.

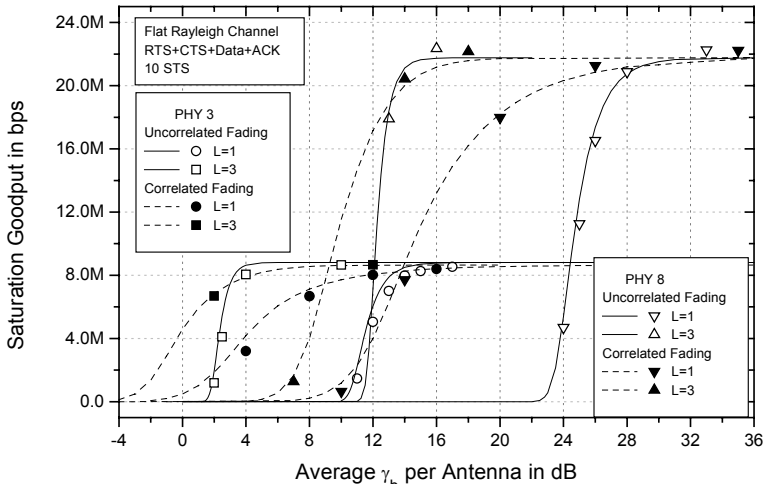

Figure 3. Comparison between analytical (straight lines) and simulation (marks) results for the goodput in bps over a Jakes correlated fading channel and a Rayleigh temporally uncorrelated fading channel. RTS/CTS Scheme.

9.3 Comparison of the Performance of Basic Access Scheme Over Correlated Fading and Uncorrelated Fading Channel

Fig. 4 shows results similar to those ones depicted in Fig. 3, except that now it is assumed the basic access scheme instead of the RTS/CTS mechanism. We again point out a good agreement between numerical and simulation results. Notice that the minimum attainable average delay does not depend on the fading be correlated or uncorrelated. The minimum delay for the PHY mode 3 is obtained with the RTS/CTS scheme and with the basic access scheme for the PHY mode 8, consistently with the remarks carried out on the results shown in Tab. 2. For uncorrelated fading, we can determine a threshold for the average SINR where the delay increases significantly when the average SINR is below of this threshold. For correlated fading, consistent with the goodput performance, this threshold is also observed, but for minor values of the average SINR.

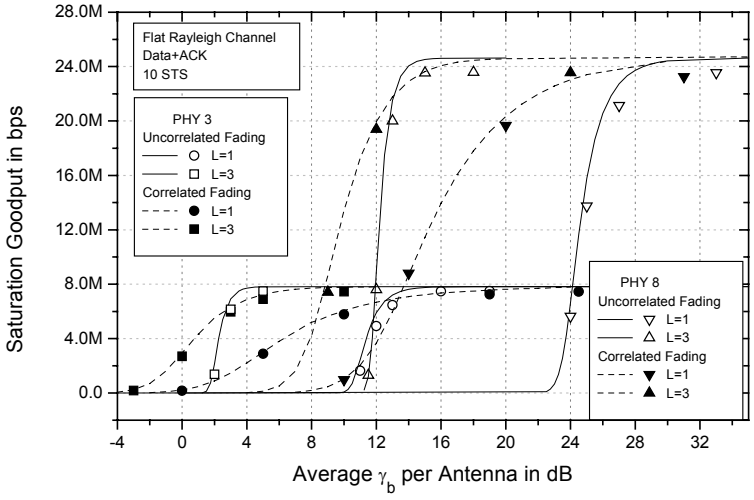

Figure 4a. Goodput in bps versus the average SINR per bit.

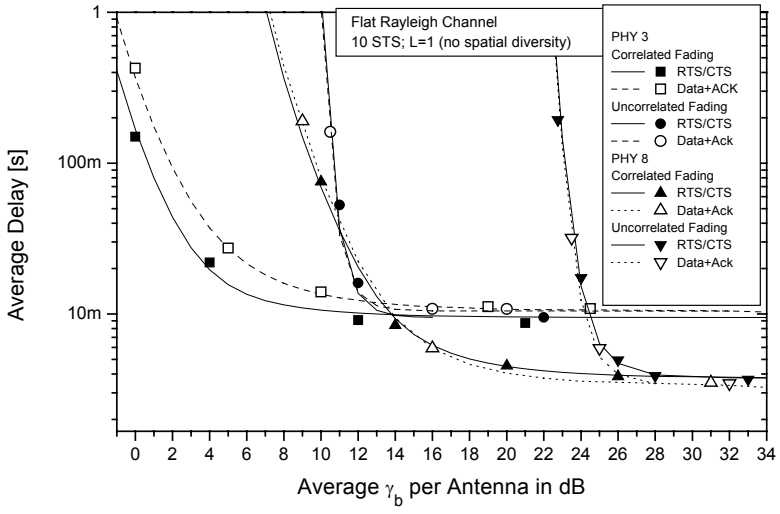

Figure 4b. Average delay in seconds versus the average SINR per bit.

Figure 4. Comparison between analytical (straight lines) and simulation (marks) results for the goodput in bps over a Jakes correlated fading channel and a Rayleigh temporally uncorrelated fading channel. Basic Mode Scheme.

Hereafter, we shall present results for IEEE 802.11a networks operating simultaneously under the basic access and RTS/CTS access schemes. It is generated MAC data payloads of *255* and *1023 octets* with equal probability (i.e. $P_{ba}=P_{rts}=0.5$). The *RTSThreshold* is set to *256 octets*.

9.4 Joint Operation of Basic Mode Scheme and RTS/CTS Access Scheme Over Correlated Fading Channel

In despite of the complexity of the MAC and PHY layers, we can verify a good agreement between analytical and simulation results for the goodput (Fig. 5a) and delay (Fig. 5b) for the joint operation of BA and RTS/CTS schemes. We can also draw the following remarks. First, we can verify that the *PHY mode 3* (QPSK with $R_c=1/2$) allows a superior performance in relation to that one obtained with the *PHY mode 1* (BPSK with $R_c=1/2$) since the QPSK signalling has a better spectral efficiency when it is implemented coherent demodulation. Notice that this also explains the better performance of *PHY mode 4* (QPSK with R_c=3/4) in relation to the *PHY mode 2* (BPSK with R_c=3/4) signalling scheme. Second, *PHY mode 5* (16QAM with $R_c=1/2$) has a better performance than the *PHY mode 2* (BPSK with $R_c=3/4$) and *PHY mode* 4.

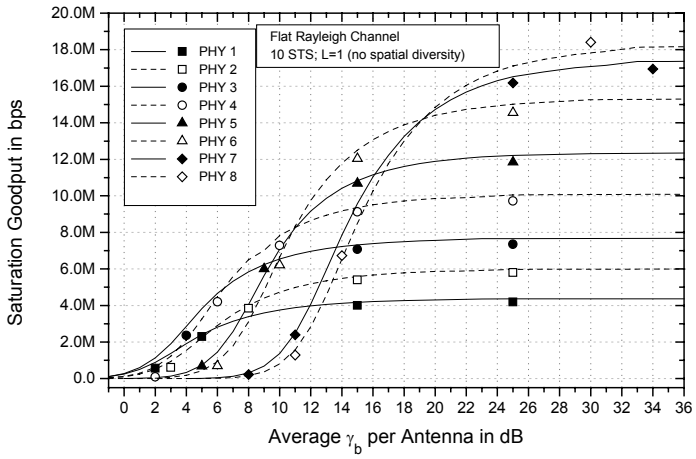

Figure 5a. Goodput in bps versus the average SINR per bit.

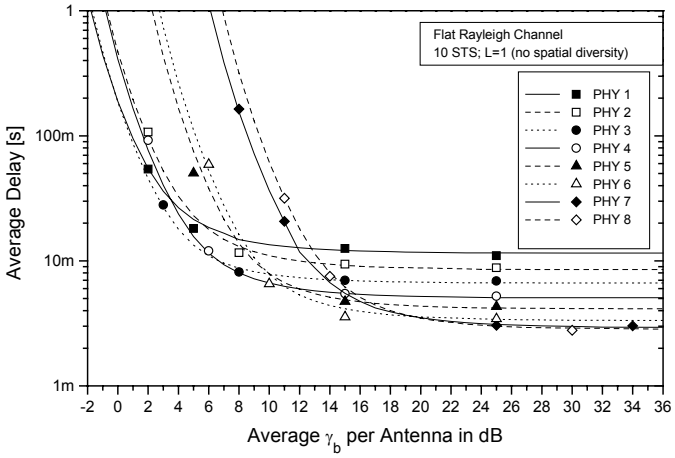

Figure 5b. Average delay in seconds versus the average SINR per bit.

Figure 5. Comparison between analytical (straight lines) and simulation (marks) results for the joint operation of basic and RTS/CTS access schemes. Correlated Rayleigh Channel.

Fig. 6 shows a comparison between analytical (straight lines) and simulation (marks) results for the following system configurations: *(1)* basic access (BA) scheme; *(2)* RTS/CTS scheme; *(3)* joint operation of BA and RTS/CTS access schemes. When it is assumed the PHY mode 3, then the better performance is obtained with the joint operation of the BA and RTS/CTS protocols. However, for the PHY mode 8, the maximum goodput is obtained with the BM scheme since the overhead of the RTS, CTS and ACK control frames is substantial in relation to the MPDU payload. Notice that in this case the greater waste of time due to collisions of MPDU frames in the basic access scheme does not counterbalance the control frames overhead.

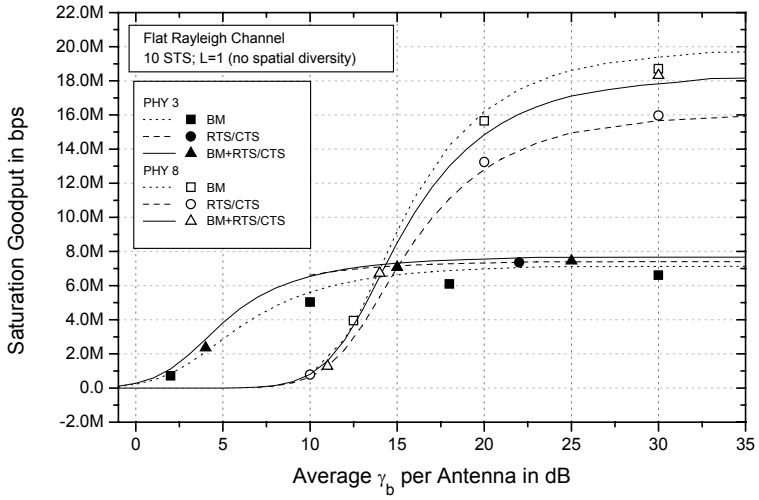

Figure 6. Comparison between analytical (straight lines) and simulation (marks) results for the goodput. Correlated fading channel.

9.5 Joint Operation of Basic Mode Scheme and RTS/CTS Access Scheme Over Uncorrelated Fading Channel

Finally, Fig. 7 is similar to Fig.5a, except that it is assumed an uncorrelated Rayleigh fading channel. Notice that the interrelations between the system performance and the different PHY modes are conceptually similar to those ones pointed out at Fig. 5a.

10. Conclusions

In this paper we have derived and validated a joint MAC and PHY cross-layer goodput saturation model that can be confidentially used to estimate first order results for the goodput and the delay of IEEE 802.11a ad hoc networks operating simultaneously under the basic access and RTS/CTS operational modes. We have considered the following: *(1)* a flat fading Rayleigh channel that is uncorrelated at symbol level and independent across the OFDM carriers; *(2)* a flat fading Rayleigh channel that is correlated at symbol level and dependent across the OFDM carriers. To sum up we strongly believe that the unified methodological approach developed here can be helpful for a widely audience of researchers, from *Computer Science* to *Telecommunications Engineering* arenas, since the results that we have developed permit a thorough understanding of a multitude of aspects involved in the challenging interrelations between complex MAC protocols and advanced PHY techniques.

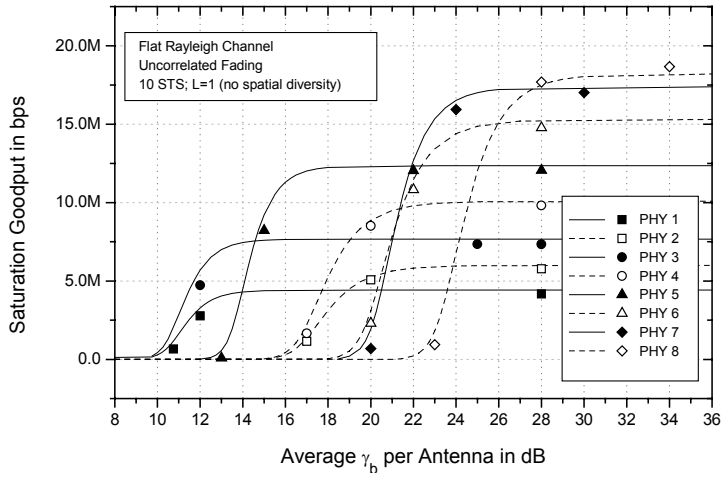

Figure 7. Comparison between analytical (straight lines) and simulation (marks) results for the joint operation of basic and RTS/CTS access schemes. Uncorrelated Rayleigh Channel.

11. References

Bianchi, G. (2000) "Performance Analysis of the IEEE 802.11 Distributed coordination function," In: IEEE Journal on Selected Areas of Communication, v.18, no. 3, pp. 535-547, March 2000.

Conan, J. (1984) "The weight spectra of some short low-rate convolutional codes," In: IEEE Trans. Communications**,** vol. 32, pp. 1050-1053, Sept. 1984.

B. P. Crow et al (1997) "IEEE 802.11 wireless local area networks," In: *IEEE Communications Magazine*, vol. 35, no. 9, pp. 116-126, Sept. 1997.

Gast, M. S. " *802.11 Wireless Networks*", New York: O'Reilly, 2002.

Haccoun, D. and Bégin, G (1989) "High-rate punctured convolutional codes for Viterbi and Sequential decoding", In: *In:* IEEE Trans. Communications**,** vol. 37, n. 11, p. 1113-1120, Nov. 1989.

Hoefel, R. P. F. (2005) "A Joint MAC and Physical Layer Analytical Model for IEEE 802.11a Networks Operating under RTS/CTS Access Scheme," In: 22^0 Simpósio Brasileiro de Redes de Computadores, May 2005.

Hoefel, R. P. F. (2006) "Goodput and Delay Cross-Layer Analysis of IEEE 802.11a Networks over Block Fading Channels," In: IEEE Consumer Communication and Network Conference, Jan. 2006.

IEEE 802.11a (1999) *"Part 11: Wireless LAN Medium Access Control (MAC) and Physical Layer (PHY) Specification – Amendment 1: High-speed Physical Layer in the 5 GHz band",* supplemented to IEEE 802.11 standard, Sept. 1999.

Proakis, J. G. (2001) "*Digital Communications",* New York, 2001.

Puersley, M. B and Taipale, D. J. (1987) "Error Probabilities for Spread-Spectrum Packet Radio with Convolutional Codes and Viterbi Decoding," *In:* IEEE Trans. Communications**,** vol. 35, n. 1, p. 1-12, Jan. 1987.

Robinson, J. W. and Randhawa, T. S. (2004) "Saturation throughput analysis of IEEE 802.11e enhanced distributed coordination function", In: IEEE J. on Select. Areas on Comm., vol. 22, no. 5, p. 917-928, June 2004.

Qiao, S. D., S. Choi and Shin, K. G. (2002) "Goodput analyzes and link adaptation for the IEEE 802.11a wireless LANs*,"* In: *IEEE Trans. Mobile Comp.*, pp. 278-292, 2002.

Yang, L. and Hanzo, L. (2000) "A recursive algorithm for the error probability evaluation of M-QAM," In: IEEE Comm. Letters, vol. 4, pp. 304-306, Oct. 2000.